doi:10.1016/S1525-0016(02)00023-0

Helper-Independent and AAV-ITR-Independent Chromosomal Integration of Double-Stranded Linear DNA Vectors in Mice

Hiroyuki Nakai,[1] Eugenio Montini,[2] Sally Fuess,[1] Theresa A. Storm,[1] Leonard Meuse,[1] Milton Finegold,[3] Markus Grompe,[2,4] and Mark A. Kay[1,*]

[1]*Departments of Pediatrics and Genetics, Stanford University School of Medicine, Stanford, California 94305*
[2]*Department of Molecular & Medical Genetics and* [4]*Department of Pediatrics, Oregon Health Science University, Portland, Oregon 97201*
[3]*Department of Pathology, Texas Children's Hospital, Houston, Texas 77030*

**To whom correspondence and reprint requests should be addressed at the Departments of Pediatrics and Genetics, Stanford University, 300 Pasteur Drive, Room G305A, Stanford, CA 94305. Fax: (650) 498-6540. E-mail: markay@stanford.edu.*

Nonviral plasmid DNA is a promising vector for achieving *ex vivo* and *in vivo* gene transfer. However, transgene expression is usually transient, especially in dividing target cells due to loss of vector genomes. Here we describe the use of naked double-stranded (ds) linear DNA as a way to insert exogenous DNA sequences into chromosomes of mouse hepatocytes *in vivo,* without helper components such as integrase or transposase. We constructed ds linear DNA vectors with or without adeno-associated virus inverted terminal repeats (AAV-ITRs), introduced them into mouse hepatocytes *in vivo* using a hydrodynamics-based transfection technique, and analyzed for vector genome integration in various ways. Surprisingly, these linear DNA molecules integrated in mouse hepatocytes *in vivo* at a level of 0.3–0.5 vector genome, or more, per diploid genomic equivalent irrespective of the AAV-ITR sequences. Our results establish a novel and simple way to engineer chromosomes *in vivo* and provide further insights into the mechanisms of recombinant AAV vector integration *in vivo*. In addition, they may provide a clue for developing new nonviral integrating gene delivery vector systems.

Key Words: naked DNA, linear DNA, adeno-associated virus, gene therapy, integration, inverted terminal repeat, mouse liver, factor IX, hereditary tyrosinemia

INTRODUCTION

Recent advances in eukaryotic expression vectors have provided various ways for efficient transfer of exogenous genes directly into *in vivo* somatic tissues of experimental animals and humans. In many *in vivo* gene transfer experiments or clinical trials, permanent transduction of target tissues is very important, especially for the treatment of inherited and acquired diseases that require persistent production of therapeutic proteins. Host chromosomal integration of vectors ensures permanent transduction in some cell types. However, most integrating vectors are derived from viruses, which require laborious and expensive procedures for production and purification and may produce undesirable products or elicit unwanted host immune response against virally encoded proteins.

Development of nonviral naked DNA-based *in vivo* integrative vectors is attractive since they have several advantages over viral-based vectors, e.g., simplicity of construction, ease of large-scale production, and cost-effectiveness. However, naked DNA vectors normally do not integrate into chromosomes *in vivo* [1,2], resulting in only transient expression of the gene of interest in many cases. As an attempt to overcome this shortcoming, we incorporated adeno-associated virus (AAV) inverted terminal repeats (ITRs) into naked circular and linear double-stranded (ds) DNA vectors and investigated whether they could integrate in mouse hepatocytes *in vivo*. The rationale for the use of AAV-ITRs is that they have been considered the sole element required for chromosomal integration by recombinant AAV (rAAV) vectors *in vitro* and *in vivo* [3,4].

In the present study, to demonstrate stable vector integration in hepatocytes *in vivo,* a hereditary tyrosinemia type I (HTI) [5,6] mouse model was used as well as normal C57BL/6 mice. HTI is an inherited fatal metabolic hepa-

1525-0016/03 $30.00

doi:10.1016/S1525-0016(02)00023-0

torenal disease caused by deficiency of fumarylacetoacetate hydrolase (FAH) [7,8]. In the absence of this enzyme, hepatocytes accumulate the toxic metabolite fumarylacetoacetate (FAA) and die in a cell-autonomous manner. FAA can be reduced with administration of 2-(2-nitro-4-trifluoromethylbenzoyl)-1,3-cyclohexanedione (NTBC) [5]. Strong positive selection for FAH-positive cells in the HTI mouse liver has been demonstrated [6,9,10] and was used for *in vivo* selection of hepatocytes with integrated vector genomes. In this system, when FAH-expressing vectors are delivered into HTI mouse livers, only FAH-positive hepatocytes with integrated vector genomes can survive and repopulate the HTI livers *in vivo*. The result is the formation of FAH-positive hepatocyte nodules and the loss of unintegrated, nonreplicating episomal vector genomes in FAH-positive hepatocytes. Our results demonstrated that simple linearization of naked DNA vectors greatly increased their integration frequency *in vivo*. In addition, the incorporation of AAV-ITRs into linear ds DNA vectors was not essential for integration but further enhanced the integration.

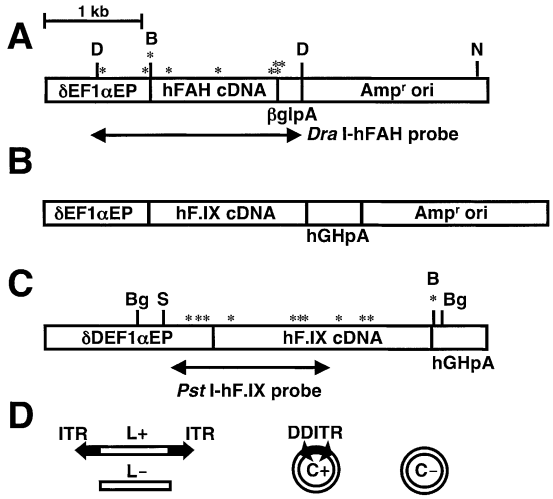

FIG. 1. Restriction enzyme maps and schematic representation of circular and linear ds DNA vectors. (A–C) Maps of hFAH or hF.IX expression cassettes used in the ds DNA vectors. Locations of restriction enzyme recognition sites and probes used for Southern blot analysis are indicated. Asterisks represent *Dpn*I recognition sites. (D) Structures of L+, L−, C+, and C− vectors. All the hFAH-expressing ds DNA vectors and the AAV-hFAH vector carried cassette (A), hF.IX-C+ and hF.IX2-C− had cassette (B), and hF.IX-L+ and L− carried cassette (C). δEF1αEP [13] and δDEF1αEP [26] are two truncated versions of the EF1α gene enhancer–promoter. Abbreviations for restriction enzymes: D, *Dra*I; B, *Bam*HI; N, *Nsi*I; Bg, *Bgl*II; S, *Sac*I.

RESULTS

Liver repopulation and genetic reconstitution in human FAH vector-injected HTI mice. We injected adult HTI mice with human FAH (hFAH)-expressing ds DNA vectors hFAH-C+, hFAH-C−, hFAH-L+, and hFAH-L− ($n = 4$ per group) via the tail vein or with AAV-hFAH via the portal vein (for vector constructs, see Fig. 1). After vector injection, the mice were kept on NTBC for 7 weeks. *In vivo* hepatocyte selection was performed by withdrawing NTBC periodically for the next 18 weeks. Liver samples collected after *in vivo* selection were analyzed for both human FAH expression by immunohistochemistry (Fig. 2) and vector genomes by Southern blot (Fig. 3). We observed liver repopulation and genetic reconstitution after *in vivo* selection in animals injected with all the vectors (Figs. 2B, 2D, 2F, 2H, 2J, 2K, 3C, and 3D). Formation of FAH-positive hepatocyte nodules demonstrated that all four naked ds DNA vector forms (hFAH-C+, C−, L+, and L−) as well as rAAV were capable of chromosomal integration in mouse hepatocytes *in vivo*. Different levels of FAH expression in different nodules but similar levels of expression in hepatocytes within each nodule, which suggested position effects of integrated transgene, also supported vector genome integration. A long *in vivo* selection period was chosen to detect even a small number of integration events, therefore this *in vivo* selection assay was not quantitative and there was no statistical difference in the integration frequencies among the groups (Fig. 2K).

Detectable integration of linear hFAH vectors in HTI mice before in vivo selection. Plasmid-derived vector genomes that have integrated into host chromosomes will lose bacterial methylation after cell division, resulting in a loss of sensitivity to the *Dpn*I restriction enzyme. Integrated vector genomes can be detected indirectly by demonstrating the presence of vector genomes resistant to *Dpn*I digestion by Southern blot analysis after DNA replication [11,32]. Six weeks after injection (i.e., prior to selection), total vector genomes (both replicated and unreplicated vector genomes) were undetectable in six of eight animals injected with the circular plasmid vectors (hFAH-C+ or C−) (Fig. 3A). Moreover, although vector genomes could be detected in two of the eight animals, these genomes were sensitive to *Dpn*I digestion (Fig. 3B), indicating that they were maintained in an episomal form. Similar to previous observations, vector genomes were undetectable in FAH-deficient animals injected with the AAV-hFAH vector (Fig. 3A) ([10] and H. Nakai *et al.,* unpublished results). It should be noted that naked supercoiled circular plasmid and AAV-hFAH vectors injected at the doses used in this study have been previously shown to be consistently maintained in the livers of normal C57BL/6 mice ([11,12] and data not shown). The discrepancy between genome numbers in FAH-deficient versus normal C57BL/6 mice suggests that FAH-expressing HTI hepatocytes can divide and lose episomal vector genomes during NTBC administration. Importantly, and in contrast to hFAH-C+, hFAH-C−, or AAV-hFAH-injected animals, vector genomes were detectable prior to selection in all the linear vector (hFAH-L+ or L−)-injected mice (Fig.

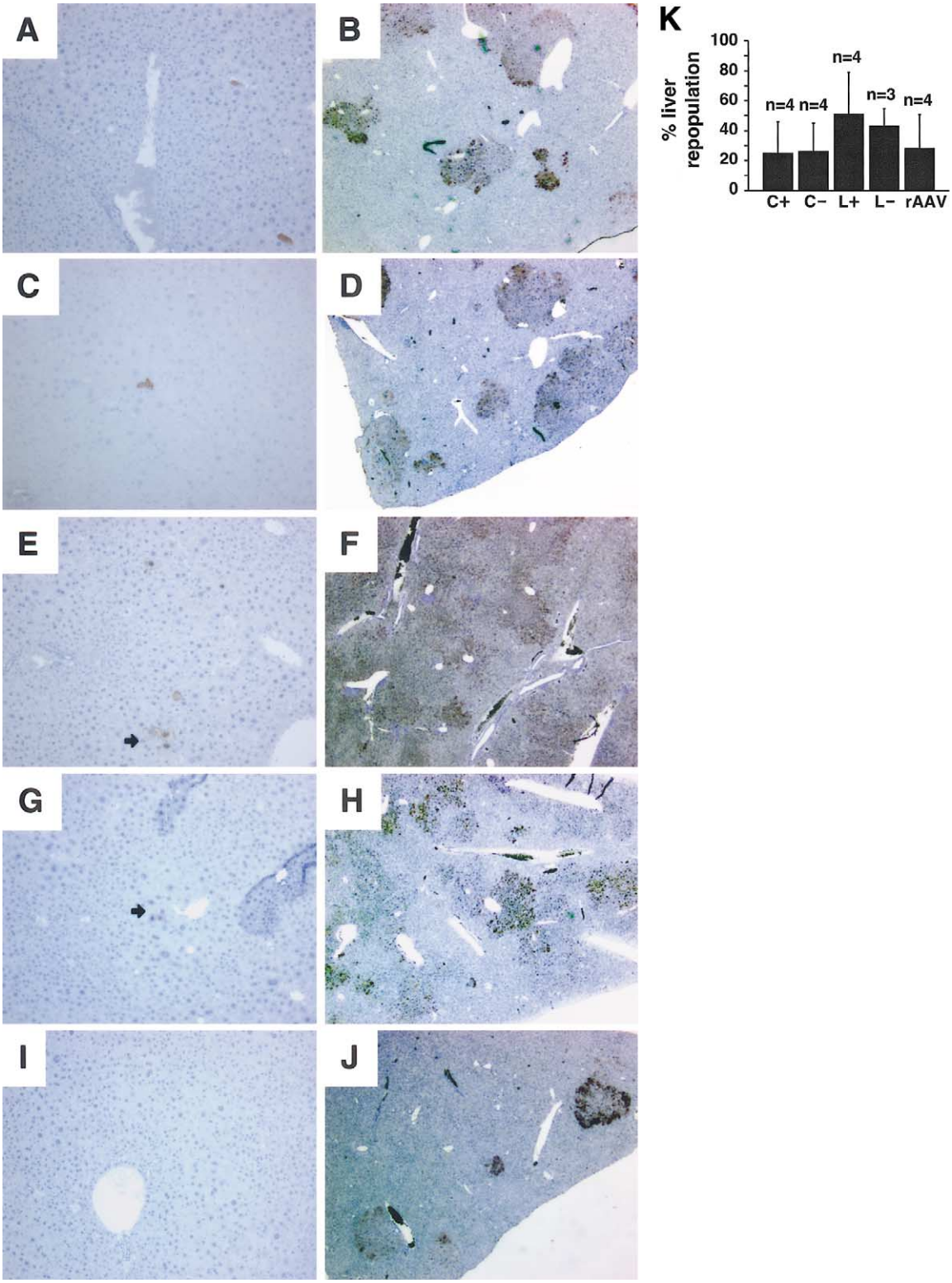

FIG. 2. Histological analysis of hFAH-expressing vector-injected HTI mouse liver. Representative results of the FAH staining of liver sections before (A, C, E, G, and I) and after (B, D, F, H, and J) *in vivo* selection. (A, B) hFAH-C+; (C, D) hFAH-C−; (E, F) hFAH-L+; (G, H) hFAH-L−; (I, J) AAV-hFAH. hFAH-expressing hepatocytes were stained brown. Black arrows indicate FAH-positive hepatocyte clusters. Original magnifications, ×10 and ×2.5 for sections before and after selection, respectively. (K) Percentage of FAH-positive hepatocytes in the livers after *in vivo* selection of 18 weeks, determined by histological analysis. Vertical bars indicate standard deviations.

doi:10.1016/S1525-0016(02)00023-0

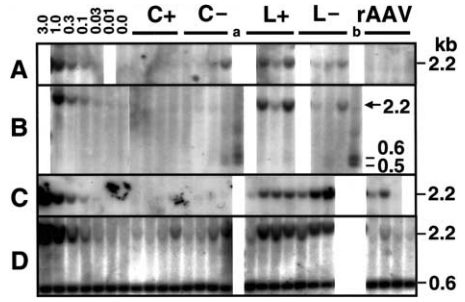

FIG. 3. Quantitation of hFAH vector genomes in HTI mouse livers by Southern blot analysis. HTI mouse livers injected with each hFAH-expressing vector were harvested 6 weeks postinjection (before *in vivo* selection, A and B) and after *in vivo* selection (C and D), and the numbers of total vector genomes (A, C, and D) and replicated vector genomes (B) were analyzed by *Dra*I digestion and a combination of *Dra*I and *Dpn*I digestion, respectively. The results from the samples collected after *in vivo* selection were verified by two Southern blots (C and D) performed independently using DNA samples extracted from different portions of the liver from individual mice. The numbers (0.0–3.0) above the lanes are hFAH vector copy number standards. Each lane represents a sample from individual mice. In B, a 2.2-kb fragment is *Dpn*I-resistant replicated vector genome, while 0.5- and 0.6-kb bands are *Dpn*I-sensitive genomes. Lanes a and b are 1.0 vector genome per diploid genomic equivalent of hFAH-C− in 20 μg of total mouse genomic DNA digested with *Bgl*II and *Dpn*I, demonstrating that the DNA was digested to completion. A *Dra*I-hFAH probe was used. In D, the blot was also hybridized with a mouse *agouti* gene probe. The signals at 0.6 kb are from the endogenous mouse *agouti* gene.

3A). Interestingly, a majority of the hFAH-L+ and L− vector genomes detected before selection were *Dpn*I resistant, indicating that they had replicated (Fig. 3B). Furthermore, hFAH-L+ vector-injected mice had a greater number of replicated vector genomes than mice injected with hFAH-L− (Fig. 3B). It should be noted that FAH-expressing hepatocytes can divide a limited number of times in HTI mice on NTBC, as mentioned above, resulting in loss of extrachromosomal vector genomes since one or two hepatocyte divisions are enough for over 90% loss of extrachromosomal vector genomes [15,32]. Taken together, these data indicate that only linear vectors could integrate into chromosomes at appreciable levels before *in vivo* selection, and the linear vector containing AAV-ITRs integrated most efficiently.

Prior to *in vivo* selection (6 weeks post-vector injection), injection of each hFAH vector resulted in very low numbers of FAH-positive hepatocytes (less than 0.1% of total hepatocytes, see Figs. 2A, 2C, 2E, 2G, and 2I). However, after injection of the linear vectors (hFAH-L+ or L−), clusters of small numbers of FAH-positive hepatocytes were frequently observed (Figs. 2E and 2G). This again suggested that hFAH-L+ or L− vector genomes integrated into hepatocytes, which subsequently divided prior to *in vivo* selection. Importantly, the total number of integrated copies of hFAH-L+ vector did not increase with *in vivo* selection in two of four mice (Fig. 3), despite the substantial increase in the number of FAH-positive hepatocytes after selection (Figs. 2E and 2F). This finding suggested that many of the integrated expression cassettes derived from linear vectors were silenced prior to *in vivo* selection. Furthermore, Southern blot analysis showed that a considerable number of integrated vector genomes after *in vivo* selection were head-to-tail, head-to-head, and tail-to-tail concatemers (data not shown), as were present before selection. Therefore it is unlikely that a small number of hepatocytes with a single integrated vector genome were responsible for repopulating the livers. Taken together, although only a small number of hepatocytes expressed FAH before selection in hFAH-L+ vector-injected mice, a relatively large proportion of hepatocytes likely contained integrated hFAH-L+ vector genomes before selection.

Isolation and analysis of integrated ds linear hFAH vectors in HTI mouse liver. We isolated vector–cellular DNA junctions (INT1 to 10, see Fig. 4) from HTI mouse livers 6 weeks after injection and analyzed them, which also supported linear vector genome integration into chromosomes before *in vivo* selection. It should be noted that the provector genomes (vector genomes integrated into chromosomes) isolated by this method may not be representative of the whole population of integration events since single-copy provector genomes are presumed to be preferentially rescued, and large concatemers are difficult to retrieve in bacteria. The integration seemed to be mediated by nonhomologous recombination with deletions at each vector end.

The effect of vector integration on the host genome was studied in six provector genomes, by aligning the junction sequences with mouse genomic sequences obtained from the mouse genome database (Figs. 4C and 4D). Integration sites were found in chromosomes 8 (INT7), 9 (INT9), 10 (INT2), 13 (INT1), 19 (INT5), and X (INT8). Deletions of mouse genomic sequences at the integration sites were commonly observed (by 33, 185, and 3664 bp). One- to 6-bp microhomology and a small nucleotide insertion were also observed at junctions. Two provector genomes (INT5 and INT8) formed complex structures and their molecular status could not be explained by a simple vector genome insertion into host chromosome with deletions (Fig. 4D). We have no definitive evidence at this time, but these structures may have been formed from the duplication of host chromosomal sequences, as we have observed in rAAV proviral vector genomes in mouse liver [13]. Alternatively, these structures might have been generated in bacteria during their isolation. If this were the case, recombination in bacteria for the construction of such rescued plasmid structures (i.e., upstream of host genome–vector genome–downstream of host genome) should have resulted in the loss of the *Kpn*I or *Avr*II site in rescued plasmid containing the provector genome. However, both INT5 and INT8 retained their *Kpn*I and *Avr*II site, respectively. Therefore, recombination in bacteria was presumed to be unlikely.

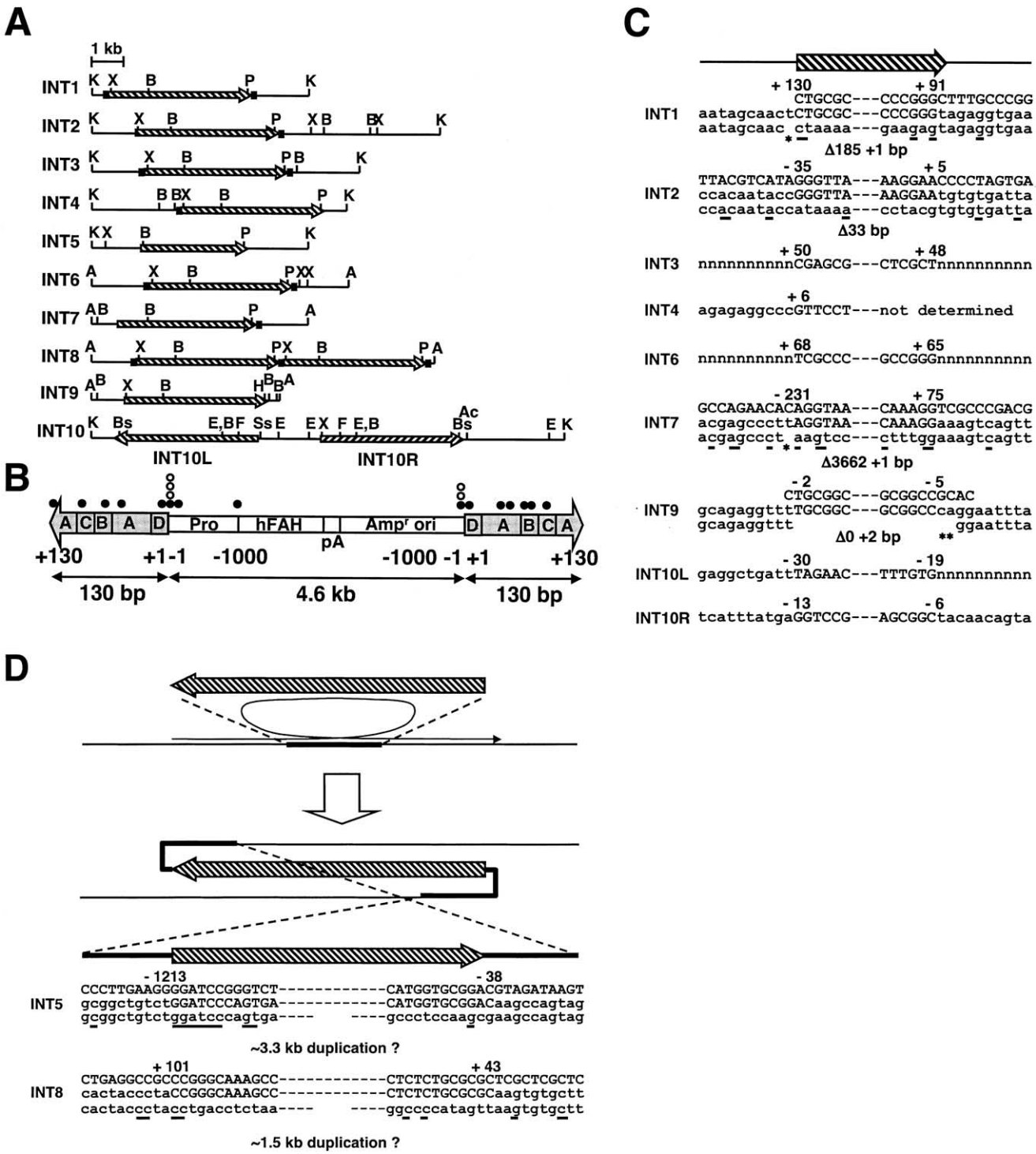

FIG. 4. Analysis of integrated vector genomes. (A) Gross structures of integrated vector genomes and their flanking mouse genomes in linear DNA vector-injected HTI mice. Hatched arrows represent the 4.6-kb transgene in the vectors. Black squares adjacent to arrows indicate the presence of remnant AAV-ITR sequences at junctions. Solid lines indicate mouse genomic DNA. INT1 to 8, and INT9 and 10 were isolated from hFAH-L+ and hFAH-L− vector-injected mouse liver DNA, respectively. K, *Kpn*I; X, *Xba*I; B, *Bam*HI; P, *Pme*I; A, *Avr*II; H, *Hind*III; Bs, *Bsr*GI; F, *Fse*I; Ss, *Sse*8387I; Ac, *Acc*I. (B) Distribution of the identified breakpoints in vector genomes. Each single open and closed circle represents one breakpoint identified in mice injected with hFAH-L− and hFAH-L+, respectively. The positive and negative numbers indicate the distance outward and inward from each end of the transgene of the vectors, respectively. Gray arrows are AAV-ITRs, and A, B, C, and D indicate the four subregions of the ITRs. (C and D) Sequences of 5′ and 3′ vector–cellular DNA junctions. Uppercase letters represent vector genomes (also shown as a hatched arrow) and lowercase letters represent mouse genomes (also shown as a solid line). In six cases, sequences of intact vector genomes and mouse genomic sequences are aligned above and below the rescued provector and flanking mouse genomic sequences, respectively. An asterisk indicates a nucleotide insertion, and underlined sequences show microhomology. Sizes of host chromosomal deletion and small nucleotide insertion are shown below each provector genome. The numbers on each breakpoint indicate the distance from each end of the transgene (see (B)). Reliable sequencing was not possible in five flanking mouse genomic sequences as shown with "n". In (D), the host chromosomal region of possible duplication is indicated with thick lines. The thin line with an arrowhead explains how the duplication is presumed to have occurred in INT5 and INT8.

doi:10.1016/S1525-0016(02)00023-0

Thus, naked ds linear DNA integration can result in deletions of host chromosomal genomic sequences (0–3.7 kb) as well as vector genomes. A BLAST search of the targeted mouse genomic sequences in GenBank and the Ensembl Mouse Genome Server revealed that INT2 and INT9 were inserted into intron 9 of the mouse Mdm2 gene (Ensembl Gene ID ENSMUSG00000020184) and intron 3 of the mouse HEMK protein homolog (Ensembl Gene ID ENSMUSG00000032579), respectively, while INT1, INT4, INT5, INT7, INT8, and INT10 did not possess homology to known mouse genes.

Integration of ds linear DNA vectors in normal C57BL/6 mice. Next, we investigated whether ds linear DNA vectors could integrate in hepatocytes of normal C57BL/6 mice, using human coagulation factor IX (hF.IX)-expressing naked ds linear DNA vectors hF.IX-L+ and hF.IX-L− and a control circular plasmid vector, hF.IX-C+ (Fig. 1). We have previously shown that hF.IX-C+ is not a substrate for appreciable integration in normal mouse hepatocytes *in vivo* [32]. C57BL/6 mice were injected with DNA vectors (hF.IX-L+, $n = 11$; hF.IX-L−, $n = 7$; and hF.IX-C+, $n = 14$), resulting in persistent and therapeutic levels of hF.IX expression with either vector ([32] and Fig. 5A). Six weeks postinjection, a 2/3 partial hepatectomy [14,15] was performed. After partial hepatectomy, each hepatocyte divides once or twice, resulting in reconstitution of the original liver mass. During regeneration, extrachromosomal, but not integrated, vector DNA is lost [15]. In addition, integrated vector genomes become resistant to *Dpn*I digestion. Therefore, the presence of *Dpn*I-resistant vector genomes could provide indirect evidence for integration unless the vector genomes replicate as episomes. Lack of episomal replication machinery of the vectors in mouse hepatocytes has been shown elsewhere [32]. As shown in Fig. 5B, the decline in human F.IX levels after hepatectomy in the hF.IX-L+ or hF.IX-L− vector-injected mice was smaller than that in hF.IX-C+ vector-injected mice. The changes in the numbers of total and replicated vector genomes determined by densitometric analysis of the blots (Fig. 6A) are summarized below. The total vector genome numbers at the time of, and 3 weeks after, partial hepatectomy were 13.88 ± 5.41 and 2.08 ± 1.61 vector genomes per diploid genomic equivalent (vg/dge) in hF.IX-L+ vector-injected mice, respectively; 7.58 ± 4.52 and 0.37 ± 0.02 vg/dge in hF.IX-L− vector-injected mice, respectively; and 5.75 ± 3.58 and 0.12 ± 0.08 vg/dge ($n = 4$ each, data not shown), respectively. The numbers of replicated vector genomes 3 weeks after hepatectomy were 0.12 ± 0.07 vg/dge in hF.IX-L+ vector-injected mice and 0.05 ± 0.02 vg/dge in hF.IX-L− vector-injected mice. Thus, the smaller decline in human F.IX levels and numbers of total vector genomes after hepatectomy in the linear vector-injected mice compared with the control circular vector-injected mice, together with the presence of *Dpn*I-resistant replicated vector genomes after hepatectomy, indicated appreciable *in vivo* integration of hF.IX-L+ and hF.IX-L− vectors. The replicated (or presumably integrated) vector genomes analyzed after hepatectomy contained head-to-tail, head-to-head, and tail-to-tail concatemers (Fig. 6B).

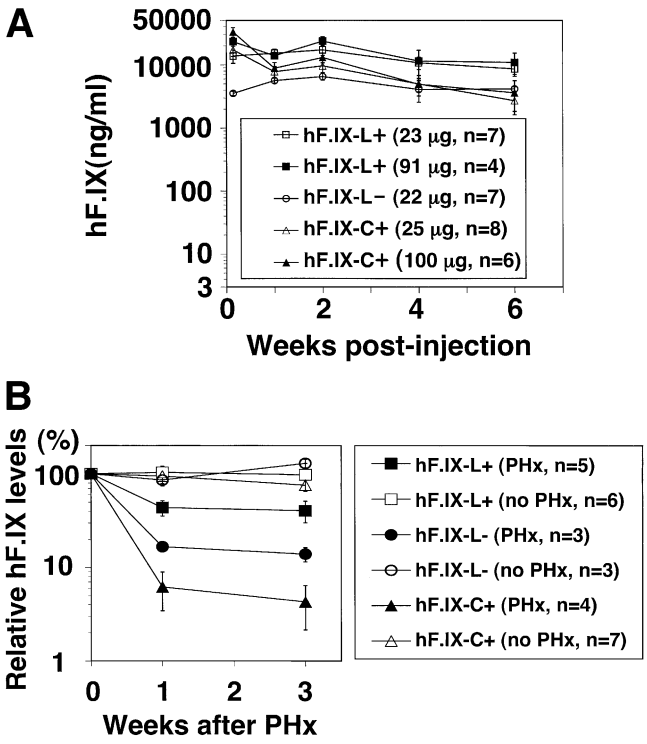

FIG. 5. Plasma human F.IX levels in ds linear or circular DNA vector-injected mice. (A) Plasma human F.IX levels after tail vein injection of human F.IX-expressing naked linear or circular DNA vector hF.IX-L+, hF.IX-L−, or hF.IX-C+. The amount of each vector (μg per mouse) and number of animals per group are shown. Each dose of vector was determined based on the molecular weight so that mice would receive the same number of, or four times more, molecules. (B) Plasma human F.IX levels after 2/3 partial hepatectomy performed 6 weeks postinjection in each individual mouse. The *y* axis represents averages of human F.IX levels relative to those at the time of hepatectomy in individual mice, shown as a percentage. Vertical bars indicate mean values ± standard errors.

In a separate experiment, we injected adult C57BL/6 mice with hF.IX-L+ (23 μg, $n = 4$) or hF.IX-L− (22 μg, $n = 3$) via tail vein and performed a combination treatment with 2/3 partial hepatectomy and administration of a hepatocyte mitogen, 1,4-bis[2-(3,5-dichloropyridyloxy)]benzene (TCPOBOP) [16] 3 weeks postinjection. This procedure was performed to increase further the amount of cell cycling after hepatectomy [17]. Three weeks later, vector genome replication in the livers was analyzed by Southern blot (Fig. 6C). Replicated vector genome numbers as determined by Southern blot analysis were 0.53 ± 0.14 and 0.33 ± 0.13 vg/dge (means ± standard deviations) in hF.IX-L+ and hF.IX-L− vector-injected mice, respectively. Because these numbers do not include integrated

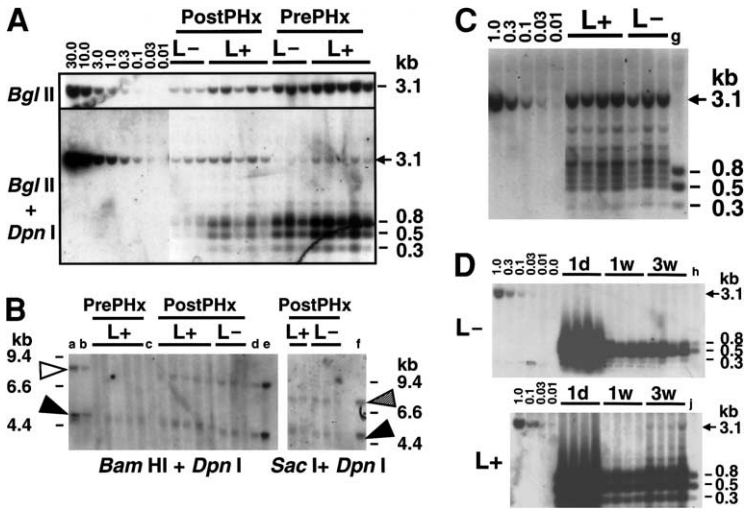

FIG. 6. Southern blot analyses of vector genomes in C57BL/6 mouse livers. (A) Quantification of total and replicated vector genomes in mouse livers injected with human F.IX-expressing linear DNA vectors at the time of (PrePHx) and 3 weeks after partial hepatectomy (PostPHx). DNA was digested with *Bgl*II or a combination of *Dpn*I and *Bgl*II. The numbers above the lanes (0.01–30.0) indicate vector genome copy number standard (vector genome per diploid genomic equivalent (vg/dge)). Each lane represents individual mice used in this study. At the bottom, the 3.1-kb fragments with an arrow represent *Dpn*I-resistant genomes, while 0.3-, 0.5-, and 0.8-kb bands are *Dpn*I-sensitive genomes. (B) Analysis of the forms of the replicated vector genomes in hF.IX-L+ or hF.IX-L− vector-injected mice at the time of (PrePHx) and 3 weeks after (PostPHx) vector injection. Molecular markers for head-to-head (open arrow) and head-to-tail forms (closed arrow) (a, b, d, and e) and tail-to-tail (hatched arrow) and head-to-tail forms (f) are 2.5 (for b and d) or 5.0 μg (for a, e, and f) of genomic DNA from a mouse injected with hF.IX-L+ (a and b) or hF.IX-L− (d, e, and f) that was digested with *Bam*HI or *Sac*I. Lane c contains 10 vg/dge hF.IX-C+ vector in 20 μg of naïve mouse genomic DNA, supporting complete digestion with *Dpn*I. *Dpn*I-only digestion or *Dpn*I–*Hpa*I digestion (*Hpa*I does not cut the vector genomes) of PrePHx samples from hF.IX-L+ vector-injected mice showed no low-molecular-weight bands indicative of extrachromosomally replicated vector genomes (data not shown). Note that only head-to-tail replicated molecules were observed in PrePHx hF.IX-L+ samples, while the replicated vector forms after partial hepatectomy included concatemers in any orientation. (C) Analysis of replicated vector genomes with *Bgl*II–*Dpn*I digestion after a combination of 2/3 partial hepatectomy and TCPOBOP administration. Lane g contains 1.0 vg/dge of hF.IX-C+ and 20 μg of naïve mouse genomic DNA, showing that fully methylated vector genomes were cut with *Dpn*I to completion. (D) Time-dependent increase in replicated vector genomes in adult C57BL/6 mice injected with hF.IX-L+. Replicated vector genomes were quantified by Southern blot analysis with a combination of *Bgl*II and *Dpn*I digestion. Lanes h and j contain the same sample as lane g in (C), showing complete digestion of the DNA. A *Pst*I-hF.IX probe was used for all the blots.

vector genomes that remained unreplicated or hemimethylated, these values still likely underestimate the true integration frequency. Nonetheless, the above results again demonstrate appreciable *in vivo* integration of naked ds linear vectors.

Although we demonstrated that ds linear DNA integrated into chromosomes in HTI and normal C57BL/6 mouse hepatocytes *in vivo* at appreciable levels, both studies relied on hepatocyte proliferation to establish integration. We therefore wanted to establish whether integration could occur in nonregenerating mouse liver. If vector genomes replicate as part of the integration process, as is often observed in the process of circular plasmid integration in cultured mammalian cells, the demonstration of amplification of vector genomes in nonregenerating liver would provide indirect evidence for *in vivo* integration unless vector genomes replicate as episomes. Southern blot analysis of nonregenerating liver DNA from mice 6 weeks after hF.IX-L+ injection showed replicated head-to-tail vector concatemers at levels of 0.06 ± 0.04 vg/dge (mean ± standard deviation) (Figs. 6A and 6B). To determine when these head-to-tail concatemers emerged, we injected adult C57BL/6 mice with hF.IX-L+ (23 μg, n = 12) or hF.IX-L− (22 μg, n = 12) DNA and analyzed liver samples from four mice in each group at 1 day, 1 week, and 3 weeks postinjection. Replicated vector genomes were quantified by Southern blot analysis. Replicated genomes emerged in a time-dependent manner and were only detected 3 weeks postinjection in hF.IX-L+ vector-injected mice at levels of approximately 0.03 vg/dge (Fig. 6D). Since hepatocytes in adult mice are not completely quiescent, it is possible that a certain population of hepatocytes could have entered S phase during the first 3 or 6 weeks, resulting in replication of integrated provector genomes. However, our results demonstrated that replicated genomes in association with hepatocyte division result in concatemers consisting of head-to-head and tail-to-tail concatemers, in addition to head-to-tail forms. The presence of only head-to-tail replicated forms in nonregenerating mouse livers injected with hF.IX-L+ suggested that the mechanism of vector genome replication was different from that associated with hepatocyte proliferation. While second-strand synthesis [18,19] and strand displacement from AAV-ITRs on extrachromosomal hF.IX-L+ might contribute to some of the replicated genomes, this would not explain the presence of fully unmethyl-

doi:10.1016/S1525-0016(02)00023-0

ated head-to-tail molecules that were completely resistant to *Dpn*I (Fig. 6B). If a majority of the replicated vector genomes were generated by second-strand synthesis, the hemimethylated *Dpn*I-resistant 3.1-kb *Bgl*II–*Bgl*II band in the blots in Figs. 6A and 6D would be negligible because there are 11 *Dpn*I sites between the two *Bgl*II sites (see Fig. 1 and Materials and Methods). Generation of fully unmethylated extrachromosomal vector genomes through the AAV-ITR requires productive genome replication, which is unlikely to occur in hepatocytes without helper functions [15]. These results are consistent with integration of hF.IX-L+ in nonregenerating mouse liver.

Two-fragment linear plasmid vectors also integrate in mouse hepatocytes in vivo. Recently Chen *et al.* [12] have reported that linearized plasmid DNA vectors could direct persistent high expression of therapeutic proteins in mouse liver, but the vector genomes likely remained as episomes since a substantial decrease in the transgene expression was observed after a surgical partial hepatectomy. They used "double-cut" plasmid vectors that were linearized such that the expression cassettes were dissociated from the bacterial plasmid backbone, and mice were then injected with both DNA species. These previous results may appear contradictory to the results presented here. To analyze whether these double-cut linear plasmid vectors can integrate in mouse hepatocytes *in vivo,* we injected C57BL/6 mice with 25 μg of hF.IX-expressing supercoiled circular plasmid vector hF.IX2-C− ($n = 6$) or double-cut linear hF.IX2-C− (i.e., hF.IX2-C− linearized with *Not*I, see Materials and Methods) ($n = 9$) via the tail vein with a hydrodynamics-based transfection technique. As previously reported by Chen *et al.* [12], the double-cut hF.IX2-C− vector-injected mice persistently expressed hF.IX in plasma, and the hF.IX levels 36 weeks postinjection were 461 ± 86 ng/ml (mean ± standard error). A two-thirds partial hepatectomy was then performed ($n = 3$ each for circular hF.IX2-C− vector-injected mice and double-cut linear hF.IX2-C− vector-injected mice). hF.IX levels in plasma of double-cut hF.IX2-C− vector-injected mice decreased by 93 ± 4% (mean ± standard error) in the hepatectomized group while in nonhepatectomized mice hF.IX levels did not change (10 ± 12% decrease) as observed by Chen *et al.* [12]. We analyzed the liver DNA at the time of, and 3 weeks after hepatectomy for the presence of replicated vector genomes by Southern blot. *Dpn*I-resistant replicated vector genomes were observed in double-cut linear plasmid-injected mice but not in circular plasmid-injected mice, indicating that double-cut plasmid could replicate presumably after integration in mouse hepatocytes *in vivo* (Fig. 7). The origin of replicated vector genomes before hepatectomy in double-cut linear plasmid-injected mice is not clear, and it is not known whether they represent replicated vector genomes in quiescent hepatocytes or hepatocytes that had entered S phase during the 32 weeks after injection. Nonetheless,

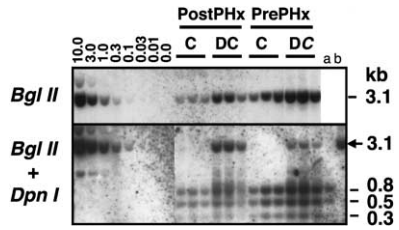

FIG. 7. Southern blot analyses of "double-cut" linear plasmid vector genomes in C57BL/6 mouse livers. Total and replicated vector genomes in mouse livers injected with circular hF.IX2-C− vector and double-cut linear hF.IX2-C− vector at the time of (PrePHx; or 36 weeks after vector injection) and 3 weeks after partial hepatectomy (PostPHx). Exactly the same analysis was performed as in Fig. 6A. Each lane represents individual mice used in this study. Both upper and lower images are from the same blot with a difference in the time of film exposure (top, short exposure; bottom, long exposure). Lane a contains 1.0 vg/dge of hF.IX2-C− and 20 μg of naïve mouse genomic DNA, showing that fully methylated vector genomes were cut with *Dpn*I to completion. Lane b is the same as 1.0 vg/dge standard. C, circular hF.IX2-C−; DC, double-cut hF.IX2-C−.

these observations indicate that in the study by Chen *et al.,* the linear DNA pieces could integrate as concatemers consisting of both the expression cassette and the plasmid backbone, and such concatemeric forms likely become transcriptionally silenced as seen in hFAH-L+ or L− injected mice in the present study. Such silenced integrated vector genomes should have a minimal contribution to the decrease in extrachromosomal transgene-derived expression after partial hepatectomy. The mechanisms of transgene silencing have not been elucidated yet; however, it may be attributed to the presence of adjoining plasmid backbone [12] or vector genome concatemerization [20].

In summary, our present study demonstrated that both ds linear and circular naked DNA vectors are capable of integration in hepatocytes *in vivo*. However, integration of circular vectors is only detectable after selection, whereas ds linear vectors integrate at appreciable levels without selection (at least 0.5 vg/dge with L+ vector), irrespective of the AAV-ITR sequences.

DISCUSSION

As shown in this study, the use of naked ds linear DNA vectors offers a simple helper-independent method for stably introducing any exogenous DNA sequence under study into mouse hepatocytes *in vivo.* In addition, incorporation of the AAV-ITRs into the vector sequence seems to enhance the capacity for *in vivo* integration further.

The present study also revealed some of the features of integrated ds linear DNA vector genomes and host chromosomal effects of integration, i.e., (1) terminals of vector genomes are commonly deleted, (2) chromosomal deletions are frequent, (3) insertions of a small number of nucleotides at junctions occur, (4) there is microhomol-

ogy between vector and chromosomal sequences, and (5) integration is mediated by nonhomologous recombination. How the deletions of host chromosomal DNA affect expression of cellular genes and exogenous transgenes requires further study.

We have been investigating the mechanisms of rAAV vector transduction in the liver and have elucidated some of the mechanisms by which incoming single-stranded rAAV vector genomes convert into various forms of ds genomes (i.e., supercoiled ds circular monomers, ds linear monomers, circular and linear concatemers, and integrated proviral forms) to establish stable liver transduction [11,13,15,21,22]. Our most recent study suggested that ds linear monomer rAAV intermediates, whose structure was the same as that of the L+ vector used in this study, not ds circular monomer rAAV genomes, whose representative form was the same as the C+ vector, play an important role in vector genome conversion [32]. In that study, in which we introduced candidates for recombinogenic rAAV intermediates (i.e., C+ and L+) into mouse hepatocytes *in vivo* using a hydrodynamics-based transfection method, we demonstrated that L+, not C+, is an intermediate for concatemerization, and C+ is not a substrate for integration. However, in that study, we had not addressed whether L+ can integrate [32]. Although it has not been established how hydrodynamics-based transfection mimics rAAV vector transduction, the similarity of the processing of vector genomes in mouse hepatocyte nuclei *in vivo* between these two systems [32] indicates that this method may be useful to study the mechanisms of rAAV vector genome conversion after vector genome entry into mouse hepatocyte nuclei. Integrative rAAV intermediates have not been identified so far, but the present study strongly suggests that ds linear rAAV monomers are possible integrative intermediates because the features of L+ integration described above are quite similar to those of rAAV proviruses found *in vitro* and *in vivo* [13,23], namely, (1) common breakage of vector genome within the AAV-ITR, (2) frequent host chromosomal deletions, (3) a small nucleotide insertion, (4) presence of microhomologies, (5) nonhomologous recombination between vector and host genomes, and (6) possible amplification of host chromosomal DNA at junctions. In addition, such similarity suggests that rAAV and ds linear DNA vectors utilize the same cellular machinery for integration, and perhaps the AAV-ITR may facilitate rAAV vector integration but is dispensable for integration itself *in vivo*.

In conclusion, we established a simple naked DNA vector-based method that can be used to insert an exogenous gene into host chromosomes of target tissues. In addition, this system may be applicable for experiments that require engineering chromosomes *in vivo* as an alternative to retroviruses or other viral-based techniques, such as gene trapping or insertional mutagenesis experiments. However, when we consider the potential for clinical applications, we need to elucidate further how the linear DNA vectors integrate into host chromosomes and how integration may affect expression of cellular proteins. Finally, elucidating the mechanisms of integration of ds linear DNA vectors *in vivo* may provide a new means of utilizing naked DNA vectors and improving current nonviral vectors.

MATERIALS AND METHODS

Construction of plasmids and rAAV vector. The vectors used are shown in Fig. 1. "C" and "L" represent circular (C) and linear (L) DNA vectors, and "+" or "−" after C or L represents vector with (+) and without (−) AAV-ITR-derived sequences. All the C+ constructs had an additional 165-bp double-D AAV-ITR (DDITR) [24,25] between a promoter and the plasmid origin of replication (ori) of the C− constructs. The DDITR consisted of a 145-bp full AAV-ITR (D-A-B-C-A) and adjoining 20-bp AAV-ITR D sequence, i.e., D-A-B-C-A-D. All the L+ constructs had a 130-bp flop-oriented AAV-ITR sequence at each end of the linear molecule, shortened by 15 bp from the terminal of the intact 145-bp ITR. All the L+ constructs were prepared by digesting corresponding plasmids with *Pvu*II, which excised L+ constructs, and purified by gel electrophoresis as described elsewhere [32].

Construction and purification of hF.IX-C+, hF.IX-C−, hF.IX-L+, and hF.IX-L− was described elsewhere [32]. Briefly, hF.IX-C+ and hF.IX-C− are agarose gel-fractionated supercoiled monomer plasmids that had a 5.2-kb DNA fragment containing the human elongation factor 1α (EF1α) enhancer–promoter (EF1αEP)-driven human coagulation factor F.IX cDNA, the human growth hormone gene polyadenylation signal (hGHpA), the prokaryotic β-lactamase gene (Amp^r), and ori. hF.IX-L+ and hF.IX-L− had the same EF1α-hF.IX expression cassette as hF.IX-C+/C−, but did not have the Amp^r and ori.

hF.IX-C− has a unique *Not*I recognition site between ori and the EF1α enhancer–promoter. To release the EF1α-hF.IX cassette from hF.IX-C− with ease, we incorporated another *Not*I recognition site between hGHpA and Amp^r in hF.IX-C−, making hF.IX2-C−. Thus, *Not*I digestion of hF.IX2-C− linearized this molecule at two sites such that the EF1α-hF.IX expression cassette was dissociated from plasmid backbone (Amp^r and ori) making a double-cut linear plasmid vector [12].

hFAH-C+ and hFAH-C− are agarose gel-fractionated supercoiled monomer plasmids, pDDITRAAV-EF1α-hFAH.AO and pEF1α-hFAH.AO.*Pvu*II, respectively. hFAH-L+ is an agarose gel-fractionated *Pvu*II–*Pvu*II DNA fragment of pAAV-EF1α-hFAH.AOS, and hFAH-L− is an agarose gel-purified pEF1α-hFAH.AO.*Pvu*II, linearized at a unique *Pvu*II site. The rAAV vector, AAV-hFAH, was produced with pAAV-EF1α-hFAH.AOS, by the triple transfection method, purified, and titered as previously described [26].

All of the naked hFAH DNA vectors and the rAAV vector carried the same DNA fragment, i.e., a 4.6-kb DNA fragment consisting of EF1αEP-driven hFAH cDNA, the human β-globin gene polyadenylation signal (βglpA), Amp^r, and ori. To construct plasmids pDDITRAAV-EF1α-hFAH.AO and pEF1α-hFAH.AO.*Pvu*II, the hF.IX cDNA and hGHpA in pDDITRAAV-EF1α-hF.IX.AO or pEF1α-hF.IX.AO.*Pvu*II [32] were replaced with a fragment containing the hFAH cDNA and βglpA. To construct pAAV-EF1α-hFAH.AOS, a DDITR sequence in pDDITRAAV-EF1α-hFAH.AO was replaced with two AAV-ITRs separated by a 1.8-kb stuffer that had been used to make pAAV-EF1α-GFP.AOSP [13]. All plasmid DNA vectors were prepared in the Dam^+ Dcm^+ strain of *Escherichia coli* Sure (Stratagene, La Jolla, Ca.) or DH10B (Gibco BRL, Gaithersburg, MD) and methylated at adenine residues in the *Dpn*I recognition sites, GATC/CTAG. None of the naked DNA vectors carried known mammalian replication elements, which was further supported by the fact that no vector genome replication was observed in association with hepatocyte division when their circular forms were delivered into mouse hepatocytes ([32], see also Results).

Animal procedures. HTI mice were the $FAH^{\Delta exon5}$ strain previously described by Grompe *et al.* [8] and inbred at the Department of Animal Care,

doi:10.1016/S1525-0016(02)00023-0

Oregon Health & Science University. Thirteen- to 16-week-old males (n = 20) were used in this study. Adult female C57BL/6 mice were obtained from The Jackson Laboratory (Bar Harbor, ME). HTI mice were provided with drinking water containing NTBC (Swedish Orphan AB, Stockholm, Sweden) at a concentration of 7.5 mg/L. HTI mice were injected with 25 μg of each naked DNA vector via the tail vein by a hydrodynamics-based liver transfection technique [27,28] or with 3.0×10^{11} particles of AAV-hFAH via the portal vein. The reason for the use of the hydrodynamics-based transfection was that this technique is the most efficient way to deliver DNA into hepatocytes of experimental animals *in vivo*. For *in vivo* selection of hFAH vector-transfected or infected HTI hepatocytes, NTBC was withdrawn for a period of approximately 2 weeks and resumed when the loss of body weight of the animals reached approximately 20–30% or they appeared ill. NTBC was withdrawn again when the body weight of the animals returned to normal. This on and off cycle was performed to prevent loss of animals and was repeated until the total period of selection reached 10 weeks. In the experiments using hF.IX DNA vectors, the amount of vector DNA (22 to 100 μg/mouse) was determined based on the molecular weight of the DNA molecule, such that mice would receive the same number of molecules (1×) or four times more molecules (4×) in comparable groups. Since there was no significant difference in either human F.IX levels or the number of vector genomes in the livers of mice receiving 1× and 4× doses within groups (Fig. 5A and data not shown), they were combined into a single group in the subsequent partial hepatectomy experiment. Portal vein injection of the rAAV vector, hydrodynamics-based *in vivo* hepatocyte transfection of naked DNA vector by tail vein injection, and partial hepatectomy were performed as previously described [14,27–30]. A hepatocyte mitogen, TCPOBOP [16], was dissolved in corn oil and orally administered at a dose of 3 mg/kg 4 h before partial hepatectomy. Compared to a 2/3 hepatectomy, in which resected liver volume increases approximately threefold, a combination of 2/3 partial hepatectomy and TCPOBOP increased the resected liver volume by approximately fivefold during a period of 3 weeks after partial hepatectomy ([17] and H. Nakai *et al.*, unpublished results). Blood samples were collected from the retro-orbital plexus of mice. All animal procedures were performed according to the guidelines for animal care at Stanford University and Oregon Health & Science University.

Measurement of human F.IX in plasma and histological analysis. Enzyme-linked immunosorbent assay specific for human F.IX was employed for the measurement of human F.IX in mouse plasma [13]. The details of the procedures for human FAH staining of liver sections were described elsewhere [6]. The percentage of liver repopulation was determined by dividing the FAH-positive areas (mm^2) by the total area of the liver section analyzed. For each liver sample, at least six different sections were analyzed (the analyzed area of each section was approximately 1 cm^2). All images were captured with a digital camera and analyzed with the software program OpenLab from Improvision, Inc.

Southern blot analysis. Total genomic DNA was extracted from mouse liver tissue and subjected to Southern blot analysis as previously described [11,13]. The vector genome copy number standards (the number of double-stranded vector genomes per diploid genomic equivalent) were prepared by adding an equivalent number of corresponding plasmid molecules to 20 μg of total DNA extracted from naive C57BL/6 mouse or HTI mouse liver. Band intensities were quantified using a G710 Calibrated Imaging Densitometer (Bio-Rad, Hercules, CA) to determine vector genome copy number per diploid genomic equivalent in each sample. To verify the integrity of the DNA samples, a mouse *agouti* gene probe [31] was used.

Replicated vector genomes in mouse liver were quantified based on resistance of vector genomes to *Dpn*I digestion. The efficiency of *Dpn*I digestion of the adenine-hemimethylated GATC/CTAG sequence under the conditions used in our study was approximately 50% [11]. Because of the incomplete digestion at hemimethylated *Dpn*I recognition sites, *Dpn*I digestion of heteroduplexes consisting of an input methylated vector genome and a newly synthesized unmethylated vector genome generates multiple partially digested bands (the longest being the fewest), since there are many *Dpn*I sites within the fragments used to quantify the replicated vector genomes (see Figs. 1A and 1C). Therefore, the vector genomes that are not digested with *Dpn*I at all are considered fully unmethylated DNA. The copy number standards for replicated vector genomes were the same as above except that they were digested with an appropriate enzyme in the absence of *Dpn*I. In some instances, the forms of replicated vector genomes were selectively analyzed by digesting DNA samples with an appropriate restriction enzyme together with *Dpn*I, which broke down *Dpn*I-sensitive unreplicated genomes into smaller fragments.

Isolation of vector–cellular DNA junctions. The strategy for isolation of 5′ and 3′ vector–cellular DNA junctions from mouse liver was based on previously published methods [13,30]. Seven micrograms of total mouse liver DNA extracted from hFAH-L+ or hFAH-L− vector-injected mice 6 weeks postinjection, a week before *in vivo* selection was started, was digested with 28 units of *Dpn*I for 4 h to remove any unreplicated extrachromosomal plasmid vector DNA. The *Dpn*I-digested DNA was then treated with calf intestinal alkaline phosphatase (CIP). Three micrograms of *Dpn*I and CIP-treated DNA was then digested with *Kpn*I or *Avr*II at 37°C for 4 h. *Kpn*I or *Avr*II does not cleave the vector genomes. The subsequent procedures to rescue integrated vector–cellular DNA junctions in bacteria were the same as previously described [13]. Isolated mouse cellular DNA sequences targeted by vectors were BLAST searched in the Ensembl Mouse Genome Server database (www.ensembl.org/Mus_musculus, February 2002 freeze) and GenBank.

ACKNOWLEDGMENTS

We thank Kazuo Ohashi and Hirotake Ono for technical assistance, Bhal Diwan for providing us with TCPOBOP, Gregory Barsh for providing us with a mouse agouti gene probe, and Clare E. Thomas for critically reading the manuscript. This work was supported by NIH Grant HL64274.

RECEIVED FOR PUBLICATION MAY 23; ACCEPTED NOVEMBER 8, 2002.

REFERENCES

1. Miao, C. H., Thompson, A. R., Loeb, K., and Ye, X. (2001). Long-term and therapeutic-level hepatic gene expression of human factor IX after naked plasmid transfer in vivo. *Mol. Ther.* **3:** 947–957.
2. Wolff, J. A., Ludtke, J. J., Acsadi, G., Williams, P., and Jani, A. (1992). Long-term persistence of plasmid DNA and foreign gene expression in mouse muscle. *Hum. Mol. Genet.* **1:** 363–369.
3. Carter, P. J., and Samulski, R. J. (2000). Adeno-associated viral vectors as gene delivery vehicles. *Int. J. Mol. Med.* **6:** 17–27.
4. Yang, C. C., *et al.* (1997). Cellular recombination pathways and viral terminal repeat hairpin structures are sufficient for adeno-associated virus integration in vivo and in vitro. *J. Virol.* **71:** 9231–9247.
5. Grompe, M., *et al.* (1995). Pharmacological correction of neonatal lethal hepatic dysfunction in a murine model of hereditary tyrosinaemia type I. *Nat. Genet.* **10:** 453–460.
6. Overturf, K., *et al.* (1996). Hepatocytes corrected by gene therapy are selected in vivo in a murine model of hereditary tyrosinaemia type I. *Nat. Genet.* **12:** 266–273.
7. Grompe, M., St-Louis, M., Demers, S. I., al-Dhalimy, M., Leclerc, B., and Tanguay, R. M. (1994). A single mutation of the fumarylacetoacetate hydrolase gene in French Canadians with hereditary tyrosinemia type I. *N. Engl. J. Med.* **331:** 353–357.
8. Grompe, M., *et al.* (1993). Loss of fumarylacetoacetate hydrolase is responsible for the neonatal hepatic dysfunction phenotype of lethal albino mice. *Genes Dev.* **7:** 2298–2307.
9. Overturf, K., al-Dhalimy, M., Ou, C. N., Finegold, M., and Grompe, M. (1997). Serial transplantation reveals the stem-cell-like regenerative potential of adult mouse hepatocytes. *Am. J. Pathol.* **151:** 1273–1280.
10. Chen, S. J., Tazelaar, J., Moscioni, A. D., and Wilson, J. M. (2000). In vivo selection of hepatocytes transduced with adeno-associated viral vectors. *Mol. Ther.* **1:** 414–422.
11. Nakai, H., Storm, T. A., and Kay, M. A. (2000). Recruitment of single-stranded recombinant adeno-associated virus vector genomes and intermolecular recombination are responsible for stable transduction of liver in vivo. *J. Virol.* **74:** 9451–9463.
12. Chen, Z. Y., Yant, S., He, C. Y., Meuse, L., Shen, S., and Kay, M. A. (2001). Linear DNAs concatemerize in vivo and result in sustained transgene expression in mouse liver. *Mol. Ther.* **3:** 403–410.
13. Nakai, H., Iwaki, Y., Kay, M. A., and Couto, L. B. (1999). Isolation of recombinant adeno-associated virus vector–cellular DNA junctions from mouse liver. *J. Virol.* **73:** 5438–5447.
14. Kay, M. A., *et al.* (1992). Hepatic gene therapy: Persistent expression of human α1-antitrypsin in mice after direct gene delivery in vivo. *Hum. Gene Ther.* **3:** 641–647.

15. Nakai, H., Yant, S. R., Storm, T. A., Fuess, S., Meuse, L., and Kay, M. A. (2001). Extrachromosomal recombinant adeno-associated virus vector genomes are primarily responsible for stable liver transduction in vivo. *J. Virol.* **75:** 6969–6976.

16. Diwan, B. A., Henneman, J. R., Rice, J. M., and Nims, R. W. (1996). Enhancement of thyroid and hepatocarcinogenesis by 1,4-bis[2-(3,5-dichloropyridyloxy)]benzene in rats at doses that cause maximal induction of CYP2B. *Carcinogenesis* **17:** 37–43.

17. Ohashi, K., Park, F., and Kay, M. A. (2002). The role of hepatocyte direct hyperplasia on lentiviral-mediated liver transduction *in vivo. Hum. Gene Ther.* **13:** 653–663.

18. Fisher, K. J., Gao, G. P., Weitzman, M. D., DeMatteo, R., Burda, J. F., and Wilson, J. M. (1996). Transduction with recombinant adeno-associated virus for gene therapy is limited by leading-strand synthesis. *J. Virol.* **70:** 520–532.

19. Ferrari, F. K., Samulski, T., Shenk, T., and Samulski, R. J. (1996). Second-strand synthesis is a rate-limiting step for efficient transduction by recombinant adeno-associated virus vectors. *J. Virol.* **70:** 3227–3234.

20. Garrick, D., Fiering, S., Martin, D. I., and Whitelaw, E. (1998). Repeat-induced gene silencing in mammals. *Nat. Genet.* **18:** 56–59.

21. Miao, C. H., *et al.* (1998). The kinetics of rAAV integration in the liver. *Nat. Genet.* **19:** 13–15.

22. Miao, C. H., *et al.* (2000). Nonrandom transduction of recombinant adeno-associated virus vectors in mouse hepatocytes in vivo: Cell cycling does not influence hepatocyte transduction. *J. Virol.* **74:** 3793–3803.

23. Miller, D. G., Rutledge, E. A., and Russell, D. W. (2002). Chromosomal effects of adeno-associated virus vector integration. *Nat. Genet.* **30:** 147–148.

24. Duan, D., Yan, Z., Yue, Y., and Engelhardt, J.F. (1999). Structural analysis of adeno-associated virus transduction circular intermediates. *Virology* **261:** 8–14.

25. Xiao, X., Xiao, W., Li, J., and Samulski, R. J. (1997). A novel 165-base-pair terminal repeat sequence is the sole cis requirement for the adeno-associated virus life cycle. *J. Virol.* **71:** 941–948.

26. Burton, M., Nakai, H., Colosi, P., Cunningham, J., Mitchell, R., and Couto, L. (1999). Coexpression of factor VIII heavy and light chain adeno-associated viral vectors produces biologically active protein. *Proc. Natl. Acad. Sci. USA* **96:** 12725–12730.

27. Zhang, G., Budker, V., and Wolff, J. A. (1999). High levels of foreign gene expression in hepatocytes after tail vein injections of naked plasmid DNA. *Hum. Gene Ther.* **10:** 1735–1737.

28. Liu, F., Song, Y., and Liu, D. (1999). Hydrodynamics-based transfection in animals by systemic administration of plasmid DNA. *Gene Ther.* **6:** 1258–1266.

29. Nakai, H., *et al.* (1998). Adeno-associated viral vector-mediated gene transfer of human blood coagulation factor IX into mouse liver. *Blood* **91:** 4600–4607.

30. Yant, S. R., Meuse, L., Chiu, W., Ivics, Z., Izsvak, Z., and Kay, M. A. (2000). Somatic integration and long-term transgene expression in normal and haemophilic mice using a DNA transposon system. *Nat. Genet.* **25:** 35–41.

31. Miller, M. W., *et al.* (1993). Cloning of the mouse agouti gene predicts a secreted protein ubiquitously expressed in mice carrying the lethal yellow mutation. *Genes Dev.* **7:** 454–467.

32. Nakai, H., Fuess, S., Storm, T. A., Meuse, L. A., and Kay, M. A. (2003). Free DNA ends are essential for concatemerization of synthetic double-stranded adeno-associated virus vector genomes transfected into mouse hepatocytes *in vivo. Mol. Ther.* **7:** .